
Research Article: Confirmation | Disorders of the Nervous System

Characterization of auditory and binaural spatial hearing in a Fragile X Syndrome mouse model

<https://doi.org/10.1523/ENEURO.0300-19.2019>

Cite as: eNeuro 2020; 10.1523/ENEURO.0300-19.2019

Received: 31 July 2019

Revised: 1 December 2019

Accepted: 20 December 2019

This Early Release article has been peer-reviewed and accepted, but has not been through the composition and copyediting processes. The final version may differ slightly in style or formatting and will contain links to any extended data.

Alerts: Sign up at www.eneuro.org/alerts to receive customized email alerts when the fully formatted version of this article is published.

Copyright © 2020 McCullagh et al.

This is an open-access article distributed under the terms of the Creative Commons Attribution 4.0 International license, which permits unrestricted use, distribution and reproduction in any medium provided that the original work is properly attributed.

1 **Title: Characterization of auditory and binaural spatial hearing in a Fragile X Syndrome**
2 **mouse model**

3 Abbreviated title: Mouse auditory spatial acuity in Fragile X Syndrome

4
5 Elizabeth A. McCullagh*^{#1,4}, Shani Poleg*¹, Nathaniel T. Greene², Molly M. Huntsman³, Daniel
6 J. Tollin^{1,2}, Achim Klug¹

7
8 1. Department of Physiology and Biophysics, University of Colorado Anschutz, Aurora,
9 Colorado, USA 80045

10 2. Department of Otolaryngology, University of Colorado Anschutz, Aurora, Colorado,
11 USA 80045

12 3. Departments of Pediatrics and Pharmaceutical Sciences, University of Colorado
13 Anschutz, Aurora, Colorado, USA 80045

14 4. Department of Integrative Biology, Oklahoma State University, Stillwater, OK 74074

15 #corresponding author

16 *co-first authors

17
18 Dr. McCullagh will soon be at Department of Integrative Biology, Oklahoma State University,
19 Stillwater, OK, USA 74078

20 Elizabeth.mccullagh@okstate.edu

21
22 7 Figures, word count: Abstract 164 words, Introduction 800 words, Discussion 2,014 words

23
24 **Conflict of Interest Statement:** The authors declare no competing financial interests.

25
26 **Acknowledgements**

27 We would like to acknowledge Dr. John Peacock for his assistance in troubleshooting the
28 various components of the behavioral set up. We would also like to acknowledge Dr. Peter
29 McCullagh and Dr. Alex Kaizer for their assistance with the statistical models used in this paper.

30
31 **Funding Sources:** Supported in part by NIH R01 DC017924 (Klug). Dr. McCullagh was funded
32 by FRAXA and NIH 3T32DC012280-05S1.

33
34 **Author Contributions:** All authors helped write and revise the manuscript. EAM, SP, NTG,
35 DJT, AK developed the ideas and methods. EAM and SP collected the data for the manuscript.
36 MMH provided the *Fmr1* animals and controls. EAM performed the statistical analyses and
37 figures for the manuscript.

38
39 **Abstract:**

40 The auditory brainstem compares sound-evoked excitation and inhibition from both ears to
41 compute sound source location and determine spatial acuity. Although alterations to the anatomy
42 and physiology of the auditory brainstem have been demonstrated in Fragile X Syndrome (FXS)
43 it is not known whether these changes cause spatial acuity deficits in FXS. To test the hypothesis
44 that FXS-related alterations to brainstem circuits impair spatial hearing abilities, a reflexive
45 prepulse inhibition (PPI) task, with variations in sound (gap, location, masking) as the prepulse
46 stimulus, was used on *Fmr1* knockout mice and B6 controls. Specifically, *Fmr1* mice show

47 decreased PPI compared to wildtype during gap detection, changes in sound source location, and
48 spatial release from masking with no alteration to their overall startle thresholds compared to
49 wildtype. Lastly, *Fmr1* mice have increased latency to respond in these tasks suggesting
50 additional impairments in the pathway responsible for reacting to a startling sound. This study
51 further supports data in humans with FXS that show similar deficits in PPI.

52

53 **Significance Statement:**

54 This is the first study to characterize auditory spatial acuity in a mouse model of FXS. We saw
55 minor differences in *Fmr1* mice compared to B6 mice in several measures of auditory acuity as
56 measured by inhibition of the startle response. *Fmr1* mice had increased latency to startle for
57 almost all conditions compared to B6 mice suggesting altered timing to acoustic cues. These
58 experiments further show that, consistent with patient report and anatomical/physiological data,
59 the auditory system is altered in a mouse model of FXS, though with some potential
60 compensation leading to a subtle behavioral impact.

61

62 **Introduction**

63 Fragile X Syndrome (FXS) is the leading monogenetic cause of autism (Penagarikano et
64 al., 2007). FXS is caused by a mutation in the gene *Fmr1* that encodes Fragile X Mental
65 Retardation Protein (FMRP). One of the hallmark symptoms of FXS, among many other
66 cognitive symptoms, is auditory hypersensitivity (reviewed in Rotschafer and Razak, 2014). An
67 imbalance of neural excitation/inhibition (E/I) is thought to underlie many pathologies in FXS
68 (Contractor et al., 2015) including those leading to auditory symptomology (Keine et al., 2016).

69 E/I imbalances in FXS extend to the auditory brainstem circuits responsible for sound
70 localization, as well as auditory cortical areas (Garcia-Pino et al., 2017; McCullagh et al., 2017;
71 Rotschafer et al., 2015; Rotschafer and Cramer, 2017). FMRP is highly expressed in the auditory
72 brainstem (Ruby et al., 2015; Wang et al., 2014; Zorio et al., 2017) leading to changes in
73 potassium channel distribution (Brown et al., 2010; Strumbos et al., 2010) that underlie changes
74 in synaptic function *in vitro* (Curry et al., 2018; El-Hassar et al., 2019; Garcia-Pino et al., 2017;
75 Lu, 2019; Wang et al., 2015). In addition, studies have shown alterations to the auditory
76 brainstem response (ABR), an *in vivo* measure of auditory brainstem activity, in *Fmr1* mice that
77 are potentially caused by these underlying changes to E/I balance and physiological activity (El-
78 Hassar et al., 2019; Rotschafer et al., 2015).

79 Binaural hearing and spatial acuity not only used for sound localization per se but are
80 also essential for communication in busy acoustic environments where several sound sources are
81 active at the same time - in the literature often labeled “cocktail party situations” (Cherry, 1953).
82 In such situations, the sound localization pathway in the auditory brainstem associates these
83 various sounds with their respective spatial channel, thereby providing the foundation for our
84 ability to follow a particular sound of interest when competing sounds are present. This
85 separation is dependent on an intricate E/I balance that starts in the auditory brainstem (reviewed
86 in (Bronkhorst, 2015; Grothe et al., 2010)). Basic encoding of sound location information is also
87 relayed through the precise balance of E/I and encoded as interaural level and timing differences
88 (ILD and ITD respectively)(Grothe et al., 2010; Pollak et al., 2002). ITDs and ILDs are
89 dependent on timing and level information from the two ears that becomes excitation or
90 inhibition within the auditory brainstem (Caird and Klinke, 1983; Goldberg and Brown, 1969;
91 Moore and Caspary, 1983; Thompson and Schofield, 2000). Therefore, impairments in the E/I
92 balance of the auditory brainstem that occur in FXS are expected to lead to impaired ability to

93 function in complex noisy acoustic environments and ITD and ILD encoding. As a signal is
94 displaced further in space from a distracting background noise, it becomes easier to discriminate
95 from the noise, this effect is termed spatial release from masking (SRM)(reviewed in Feng and
96 Ratnam, 2000). Despite the substantial alterations to the auditory brainstem in FXS, it has never
97 been clearly shown, beyond patient report and surveys, that mice or humans with a mutation in
98 *Fmr1* have impairments in their ability to localize sound in normal listening or complex acoustic
99 environments (Baranek et al., 2008, 2002; Rogers et al., 2003).

100 This study tests the hypothesis that mice with a mutation in the *Fmr1* gene have a
101 functional deficit in binaural hearing despite a normal range of auditory hearing ability. Binaural
102 hearing ability was assessed using a reflexive prepulse inhibition (PPI) paradigm, where a
103 change in the sound source location served as the prepulse, a method described previously for
104 mice (Allen and Ison, 2010) and guinea pigs (Greene et al., 2018). The acoustic startle response
105 is a reflexive whole-body response elicited by a very brief, but loud impulse noise. PPI consists
106 of modification of the acoustic startle response by pairing the startle eliciting stimulus with a
107 preceding stimulus, the prepulse, that inhibits the startle response by providing a cue to the
108 impending startle (Young and Fechter, 1983). PPI is a useful tool for measuring deficits in
109 cognitive disorders such as autism, FXS, or schizophrenia since it is reflexive and independent of
110 cognitive ability (Young and Fechter, 1983). It has been shown previously, with conflicting
111 results, that mice and humans with *Fmr1* mutations have impaired PPI (Chen and Toth, 2001;
112 Frankland et al., 2004; Hessel et al., 2009; Nielsen et al., 2002; Thomas et al., 2012; Veeraragavan
113 et al., 2012) suggesting altered sensorimotor gating. We use a similar PPI paradigm, but with
114 cues to specifically target spatial hearing ability (gap in sound, speaker swaps and spatial release
115 from masking), to test the hypothesis that behavioral impairments result from altered signaling in
116 the brainstem sound localization circuits. We show subtle changes in *Fmr1* mice responses to
117 spatial auditory stimuli, quantified as reduced PPI, reduced detection of prepulses compared to
118 wildtype animals, and increased response latencies to startling sounds.

119 **Materials and Methods**

120 All experiments complied with all applicable laws, NIH guidelines, and were approved by the
121 University of Colorado Anschutz IACUC.

122 *Subjects*

123
124 All experiments were conducted in either C57BL/6J background (wildtype) or hemizygous male
125 and homozygous *Fmr1* knockout strain maintained on the background (commercially available
126 through Jackson Laboratory, Bar Harbor, ME, *Fmr1* stock number 003025, B6.129P2-
127 *Fmr1*^{tm1Cgr}/J (Consortium et al., 1994), C57BL/6J stock number, 000664). Forty-six total mice
128 were used, exact number of animals used per experiment are listed in the figure legend and
129 corresponding results sections. The results are based on experiments conducted in both male (N
130 = 30) and female (N = 16) wildtype and *Fmr1* knock out mice. No significant differences were
131 observed between sexes, and data for males and females were combined. Animals were
132 genotyped regularly using Transnetyx (Cordova, TN). Mice used in these experiments were all
133 adult animals and varied in age between 55 and 167 days old. Age was not significantly different
134 between the two groups ($p = 0.96$, *Fmr1* mice 83.1 ± 4.3 days old, wildtype mice 83.4 ± 4.7
135 days old). Each animal was weighed after completion of data collection. Animal weights varied
136 between 13-37 g, and generally increased with age. On average, *Fmr1* mice tended to weigh less
137 (23.5 ± 0.75 g) than wildtype animals (25.8 ± 0.43 g) ($p = 0.01$). Pinna morphology was
138

139 measured using methods as described in Anbuhl et al., 2017 by measuring the height and width
140 of each ear and estimating the effective diameter (square root of the height x width). There was
141 no significant difference in pinna morphology between B6 and *Fmr1* animals ($p = 0.9026$,
142 diameter 8.79 ± 0.36 B6, 8.84 ± 0.21 *Fmr1*).

143

144 *ABR Audiogram*

145 ABR recordings were conducted using methods similar to those described previously (Anbuhl et
146 al., 2017). Briefly, a devoted cohort of mice (7 mice of each genotype 132 ± 2.8 days old B6,
147 117.9 ± 4.3 days old *Fmr1* of both sexes) were anesthetized (60mg/kg Ketamine +
148 10mg/kg Xylazine for initial anesthesia and 25mg/kg Ketamine + 12 mg/kg Xylazine), and
149 placed on a heating pad in a small sound-attenuating chamber (ETS-Lindgren). Stimuli
150 presentation and generation as well as evoked potentials recording were conducted through
151 custom MATLAB (Mathworks Inc. Natick, MA) software interfacing with an RME
152 (Haimhausen, Germany) Fireface UCX sound card (operating at a sampling rate of 44.1 kHz).
153 Stimuli were presented through calibrated (Beutelmann et al., 2015) Etymotic (Elk Grove
154 Village, IL) ER10B+ ear coupling tubes, and presented by ER2 earphones using standard sound-
155 delivery tubes. Evoked potentials were made with platinum subdermal needle electrodes (F-E2-
156 12 electrodes; Grass Technologies, West Warwick, RI) simultaneously at the apex, and behind
157 each pinna (active), referenced to the nape of the neck, with a hind leg ground. Signals were
158 amplified and digitized by a Tucker Davis Technologies low impedance headstage (RA4LI) and
159 preamplifier (RA4PA), further amplified digitally (10,000x), and output as an analog signal by a
160 multi-I/O processor (RZ5). ABRs were recorded in response to 1000 repetitions of short (5 ms)
161 tone-burst (4, 8, and 16 kHz) stimuli, gated on and off with 1 ms linear ramps, and presented at a
162 rate of ~14 per second. Frequencies of the ABR stimuli spanned the effective bandwidth of the
163 auditory stimuli used for behavioral testing (see next section). Stimuli included interleaved
164 presentations of left and right monaural, as well as binaural stimulus presentations. Responses
165 were initially recorded for 90 dB SPL stimulus presentations, then for progressively lower levels
166 (in 10 dB SPL steps) until threshold was found. Threshold was determined as the average
167 between when a waveform was present and the next dB SPL step in which a discernable ABR
168 signal appeared. Responses were analyzed by assessing for the lowest level eliciting a detectable
169 evoked potential in any of the three recorded channels.

170

171 *Apparatus*

172 Experimental conditions and apparatus are previously described in Greene et al., 2018 but
173 are also briefly described here. All experiments were conducted in a double-walled sound
174 attenuating chamber (IAC Bronx, NY) lined with acoustical foam to reduce echoes. The animal
175 was snugly placed, in order to ensure the animal was forward-facing, in a custom-built
176 acoustically transparent steel-wired cage attached to a polyvinyl chloride post anchored to a
177 flexible polycarbonate platform with an accelerometer (Analog Devices ADXL335 Norwood,
178 MA) to capture startle responses. All animals were tested in the dark using a closed-circuit
179 infrared (IR) camera to monitor movement and proper orientation of the animal. When the
180 animal was placed snugly into the chamber with the steel lightly compressed around its body, the
181 animal maintained its forward-facing position and was unable to turn around. The cage with the
182 animal was then always oriented towards the center loudspeaker. A diagram with the
183 experimental apparatus is shown in (Greene et al., 2018). The chamber consisted of an array of
184 25 loudspeakers (Morel MDT-20 Ness Ziona, Israel) placed horizontally in a 1 m radius

185 semicircular boom at 7.5° intervals from -90° (right) to +90° (left) in front of the animal from
186 which pre-pulse stimuli were presented. Startle stimuli were presented from a Faital Pro HF102
187 compression driver (Faital S.p.A. San Donato Milanese, Italy) placed ~ 35cm (from the base of
188 the platform) directly above the cage and amplified using an Alesis RA150 (Cumberland, RI).

189 Stimuli were generated and responses recorded from three Tucker-Davis Technologies
190 (TDT Alachua, FL) RP 2.1 Real-Time processors using custom written MATLAB (Mathworks
191 Natwick, MA) software. The startle stimuli were 20ms broad-band noise bursts generated by one
192 of the RP2.1 processors and presented at 110dB SPL (unless otherwise stated such as in the
193 startle threshold experiments). Carrier stimuli (CS) were broadband-noise generated by a second
194 RP2.1 and presented continuously (unless otherwise noted) during testing. In the speaker swap
195 experiment the broad-band noise was high-pass filtered (4 kHz cutoff) with a 100th order FIR
196 filter. Because the Morel MDT-20 loudspeakers begin to roll off at 20 kHz the effective
197 bandwidth of the noise stimuli was ~4-20 kHz. The CS was presented from one speaker at a time
198 and had the ability to be switched by two sets of TDT PM2Relay power multiplexers controlled
199 by the RP2.1s. Attenuation of the signals and startle stimuli was achieved using TDT PA5
200 programmable attenuators. Vertical movement of the polycarbonate plate on which the
201 accelerometer was mounted was detected as the voltage output, sampled at 1kHz by one of the
202 RP2.1s. Startle response amplitude was calculated as the root mean square (RMS) of the
203 accelerometer output in the first 100ms after the delivery of the startle stimuli, and startle latency
204 was calculated as the delay between the startle stimulus onset and the time at which the
205 accelerometer output exceeded three standard deviations of the 100 ms immediately preceding
206 the startle stimulus presentation.

207 208 *Experimental Conditions*

209 Four types of experiment were conducted on most of the animals, startle threshold, gap
210 detection, speaker swap, and spatial release from masking (similar to experiments performed in
211 (Allen and Ison, 2010; Greene et al., 2018). The first repetition within a condition was excluded
212 from analysis and all conditions were presented at least four times per experiment with most
213 experiments containing six or more trials per condition. Most of the animals were tested once in
214 each experiment; however, some mice were not subjected to acoustic startle threshold testing to
215 reduce overall data collection time. The order of each of the four types of experiments was
216 pseudo-randomized for each animal and each animal was only tested once per experiment
217 (startle, gap, etc.). Total time of testing was around three hours per animal, and all conducted on
218 the same day. The inter-trial interval (ITI time between trials) was uniformly distributed between
219 15-25 s in 1 s increments to prevent the animal from acclimating to the time of startle. For all
220 experiments excluding the startle threshold, the startle stimulus was presented at 110 dB SPL.
221 Order of prepulse conditions were pseudo randomly presented for each experiment.

222 223 *Experiment 1: Startle Threshold*

224 Startle threshold was assessed by varying the intensity (for most animals between 60-
225 120dB SPL in 10dB steps) of the startle eliciting stimulus, presented with the overhead startle
226 speaker and recording their acoustic startle response (ASR) through the cage-mounted
227 accelerometer. Startle responses were assessed in the presence of a 70dB SPL background noise
228 played continuously from the speaker directly in front of the animal (0°). Presentation of these
229 conditions were limited to three to five repetitions to ensure that the animal had a robust startle
230 response while minimizing the duration of testing.

231

232 *Experiment 2: Gap Detection*

233 The ability of animals to detect a short quiet period in a continuously noisy background
234 was similarly assessed by presenting a broadband noise from the speaker directly in front of the
235 animal (0°). A 20 ms gap in the noise (the pre-pulse) was introduced before the startle eliciting
236 stimulus with interstimulus-intervals (ISI, time between the stimulus (gap) and startle eliciting
237 stimulus)(Figure 3A) of 1, 2, 5, 10, 20, 40, 80, 160 and 240 ms from the onset of the gap. A
238 subset of animals were only tested with 10, 20, 40, 80, 160 and 240 ms ISIs. Responses were
239 assessed for ten repetitions of each ISI, presented pseudo randomly in a block-wise fashion. Two
240 control condition trials, consisting of the continuous broadband noise with no gap preceding the
241 startle-eliciting stimulus, were included in each repetition block.

242

243 *Experiment 3a: Fixed 90° angle speaker swap with variable inter-stimulus interval (ISI)*

244 The optimal ISI for speaker swap detection was assessed by swapping the source speaker
245 (the prepulse) of a continuous broadband noise (70 dB SPL) 90° symmetrically across the
246 midline (Figure 4A). The background noise was initially played from the speaker -45° (right)
247 with respect to the animal and swapped with to the speaker +45° (left) of the animal some ISI
248 prior to the startle-eliciting stimulus. Startle responses were assessed for five repetitions of 1, 2,
249 5, 10, 20, 30, 40, 80, 100, 150, and 300 ms ISIs, presented randomized in a blockwise fashion.
250 Two control conditions, where no speaker swap occurred (i.e. the noise was continuously played
251 from the initial speaker at -45°), were included in each repetition block. The ISIs for gap and
252 speaker swap detection may be different as well as number of repetitions needed and therefore
253 different ISIs and number of repetitions were presented for experiments 2 and 3a.

254

255 *Experiment 3b: Variable angle speaker swap with 20 ms fixed ISI*

256 Minimum audible angle was similarly assessed using a speaker swap paradigm. The
257 animal orientation was maintained at 0° (center) as described above to test responses to sounds
258 swapped across the midline and assess minimum audible angle detection ability. The prepulse
259 was a change in the source of a high-pass noise (cut off below 4kHz) between two matched
260 speakers separated by 7.5°, 15°, 30°, 45°, and 90° symmetrically (except for 7.5°) across the
261 midline, in both directions (left to right and right to left). ISI was set at 20 ms between
262 presentation of the prepulse (speaker swap) and startle-eliciting stimulus. The ISI was set in this
263 experiment to reduce the length of the overall experimentation time and based on the results
264 from experiments 3a and 2 showing that an ISI of 20ms is optimal for eliciting PPI. Startle
265 responses were assessed for eight presentations of each condition (N = 10 since swap angle and
266 direction co-vary), and one control condition (the high pass noise presented from the starting
267 speaker, but no swap to the matched speaker) for each starting speaker (N=10), were presented
268 randomized within repetition blocks.

269

270 *Experiment 4a: Detection threshold for Spatial Release from Masking*

271 The detection threshold of the signal used in a spatial release from masking (SRM), i.e.
272 the ability of mice to detect a signal in a continuous 70 dB SPL broadband masking noise,
273 presented from the center speaker (0°), was assessed by varying the intensity of the “signal”
274 speaker presented adjacent to the center speaker (7.5°, SRM threshold, Figure 6A). The ISI was
275 set at 20 ms from the onset of the prepulse to the startle eliciting stimulus. The “signal” was a
276 100 ms duration multi-tone complex with a 4kHz fundamental frequency and overtones at octave

277 spacing up to 32kHz (4 octaves). The intensity of the signal was varied by decreasing the signal
278 level by 9, 12, 15, 18, 21, 24, and 27 dB attenuation relative to the full scale (~83.5 dB SPL),
279 with a TDT PA5 programmable attenuator. Two control conditions (in which the masking noise
280 was presented continuously with no “signal” prepulse presented) were included in each of five
281 randomized trial blocks.

282

283 *Experiment 4b: Speaker Swap Spatial Release from Masking*

284 SRM was assessed by varying the location of the signal speaker at two levels determined
285 based on preliminary results from the detection threshold task. In this task, the same “signal” as
286 in Experiment 4a was presented at 15 or 24 dB attenuation (from ~83.5 dB SPL, Figure 7A),
287 from speakers at 7.5°, 15°, 30°, 45°, and 90° (to the left or right) relative to center (0°) at a
288 constant ISI of 20 ms. Two control conditions (in which the masking noise was presented
289 continuously with no “signal” prepulse presented) were once again included in each randomized
290 repetition block (of five).

291

292 *Data Analysis*

293 The ASR was assessed as the RMS output of the accelerometer, amplified by 25dB in the
294 100 ms following the startle eliciting stimulus presentation. The units of the ASR are reported as
295 arbitrary voltage units that are proportional to meters/second since the output of the
296 accelerometer was not explicitly calibrated (though it was held constant throughout data
297 collection). The mean ASR was calculated for each animal, with the first presentation of each
298 condition excluded to exclude initial adaptation to the startle. Most responses were quantified as
299 prepulse inhibition (PPI), calculated as 1 minus the ratio of the mean prepulse ASR during each
300 prepulse condition (ASR_p) to the mean ASR during the corresponding control condition(s)
301 (ASR_c), recorded for each session: $PPI = 1 - [ASR_p/ASR_c]$. A PPI of 0 corresponds to an ASR_p
302 equal to ASR_c suggesting no detection of the prepulse, whereas both positive PPI, indicating a
303 reduction in ASR, and negative PPI, indicating an increase in ASR, suggest that the prepulse was
304 detected and modified the animal’s startle response. Figures were generated in R (R Core Team,
305 2013) using ggplot2 (Wickham, 2016). Data were analyzed using a mixed effects model to
306 account for repeat observations within one animal (lme4 (Bates et al., 2014)) with genotype and
307 conditions (dB SPL, ISI, angle, ABR threshold, etc.) as fixed effects, and animal as a random
308 effect. It was expected that there would be no differences between some conditions where the
309 prepulse was not detectable. Therefore apriori, independent of results from fixed effects (i.e. no
310 difference in main effect of genotype), it was determined that estimated marginal means
311 (*emmeans*, (Lenth, 2019)) were going to be used to make pairwise comparisons between
312 genotype and condition or replicate and condition. A Tukey method for multiple comparisons
313 was implemented for these contrasts using *emmeans*. A zero-intercept model was used to
314 compare genotypes to a PPI value of zero (to determine detection of the sound prepulse). T-tests
315 used Satterthwaite’s method for comparing the multiple levels of ISI across genotype
316 (Kuznetsova et al., 2017). Animal weight and age were compared between the two genotypes
317 using a two-tailed t-test and data are presented as mean \pm standard error. Tables 1-3 show mean,
318 standard error, median, interquartile range (IQR) and p-values for each experiment. Red values
319 in Table 2 indicate conditions where PPI was greater than zero. Where values are indicated as
320 statistically significant between the two genotypes, * indicated a p-value of < 0.05 , ** = $p <$
321 0.01 , and *** = $p < 0.0001$. Figures were prepared for publication using Adobe Photoshop and
322 Adobe Illustrator (Adobe, San Jose, CA).

323

324 **Results**325 *ABR audiogram*

326 Hearing range for *Fmr1* and B6 mice was determined through presenting tones of varying
327 frequency (4, 8, 16 kHz) and recording the threshold of the auditory brainstem response (ABR).
328 These frequencies span the bandwidth of the noise stimuli used for behavior. There was a main
329 effect of genotype ($p = 0.043$) indicating that the ABR thresholds were different between *Fmr1*
330 and B6. Posthoc analysis showed that the two genotypes were no different for 4 and 8 kHz but
331 that *Fmr1* mice had increased ABR thresholds at 16 kHz compared to wildtype (Figure 1, Table
332 1).

333

334 *Experiment 1: Startle Threshold*

335 Animals were initially tested to determine their response threshold to acoustic startle
336 stimuli. This was done both to characterize the responses of *Fmr1* mice and ensure that all
337 animals had a robust startle response with increasing intensity of sound. Startle amplitude is
338 reported in units of arbitrary volts (output of the accelerometer) that are an uncalibrated measure
339 proportional to acceleration. Startle sounds were 20 ms in duration and varied in intensity
340 between 60 and 120 dB SPL presented randomly in 10 dB SPL steps, in the presence of
341 continuous 70dB SPL broadband noise (presented from the speaker directly in front of the
342 animal) (Figure 2A). All animals were tested with intensities ranging from 80-120 dB SPL. Two
343 additional levels (60 and 70 dB SPL) were tested in a subset of animals (6 B6, 8 *Fmr1*) to ensure
344 that animals are not startled at lower intensity sounds. There was no difference between
345 genotypes for either startle amplitude (Figure 2B, $p = 0.4074$) or latency (Figure 2D, $p = 0.8331$).
346 Startle responses increased and latency decreased with increasing stimulus level in both
347 genotypes, indicating that animals had no trouble detecting the startle stimulus and had a robust
348 startle response. The magnitude of the startle responses for both B6 and *Fmr1* animals plateaued
349 (threshold) around 100dB SPL and therefore the startle stimulus was set at 10 dB above this
350 threshold (110 dB SPL) for the remainder of the experiments.

351 When individual animal weights were used to calculate the force of each startle response
352 (in arbitrary units proportional to Newtons), significant differences were observed between
353 genotypes at 100 ($p = 0.0321$) and 110 ($p = 0.0224$) dB SPL with *Fmr1* mice showing reduced
354 startle force compared to wildtype (Figure 2C). This could be due to a reduced muscle tone in
355 *Fmr1* animals or some other factor, neither of which are explored further in this study. To
356 account for differences in animal weight and reduced startle force, responses are normalized to
357 the baseline startle amplitude when calculating PPI (see methods).

358

359 *Experiment 2: Gap Detection*

360 Recent data has shown that impairments in gap detection may be caused by underlying
361 changes to excitation-inhibition balance (E/I) in the inferior colliculus (IC) (Sturm et al., 2017),
362 suggesting that gap detection may be used to probe the E/I balance in the auditory system. This
363 E/I balance is known to be altered in FXS (Garcia-Pino et al., 2017; McCullagh et al., 2017;
364 Rotschafer et al., 2015). We tested 42 animals (20 B6 and 22 *Fmr1*) in a gap detection paradigm
365 with a 20 ms quiet gap in broad band noise (prepulse) followed by a startle eliciting stimulus at
366 varying inter-stimulus interval (ISI) times (1-240 ms) between the prepulse and startle eliciting
367 stimuli (Figure 3A, B). A subset of animals were only tested at 10-240 ms ISIs (8 B6, 8 *Fmr1*).
368 There was no main effect of genotype ($p = 0.2011$) at all durations of ISI, however there were

369 significant differences between B6 and *Fmr1* animals at 10 ms ($p < 0.05$) and 20 ms ($p < 0.01$)
370 ISIs (Figure 3B). In addition, *Fmr1* mice were slower to startle at all ISIs (as indicated by
371 increased startle latency, (main effect of genotype, $p = 0.00000255$)), except 10 ms and 20 ms,
372 compared to B6 mice (Figure 3C). Both genotypes did not show PPI significantly different from
373 zero for ISI of less than 1 ms ($p = 0.45$ B6 and $p = 0.91$ *Fmr1*), and additionally at 2 ms ($p =$
374 0.14) for *Fmr1* mice suggesting a lack of detection of the prepulse with these short ISIs. These
375 data suggest that not only do *Fmr1* mice have decreased PPI compared to wildtype at optimal
376 ISIs but are also consistently slow to startle under most conditions, where in contrast, B6 mice
377 show modulations to latency based on ISI.

378

379 *Experiment 3a: Varying ISI with 90° Speaker Swap*

380 The gap detection test suggests that *Fmr1* mice demonstrated deficits in temporal
381 auditory processing, next we wanted to determine if *Fmr1* mice also have deficits in spatial
382 auditory processing. The first step to determining whether *Fmr1* mice have spatial hearing
383 deficits is to establish the optimal ISI for detection of a spatial speaker swap. In this task, the
384 prepulse was a speaker swap of broadband noise from one speaker 45° to the right of the animal
385 to the symmetrical speaker 45° to the left of the animal (90° total angle), with varying ISIs
386 between the prepulse and startle eliciting stimuli (Figure 4A). There was no main effect of ISI on
387 genotype ($p = 0.1068$). However, *Fmr1* mice had reduced PPI of their startle compared to B6
388 mice at 20 ms and 30 ms ($p < 0.05$) ISI after the 90° speaker swap (12 B6, 14 *Fmr1* mice, Figure
389 4B). In addition, *Fmr1* mice showed an increased latency to startle compared to B6 at all ISIs
390 except 1 ms and 2 ms (Figure 4C, main effect $p = 0.0000007913$). These data suggest that at ISIs
391 that elicited some of the highest PPI for B6 animals (also similar ISIs that showed a deficit in the
392 gap detection test), *Fmr1* mice showed reduced PPI compared to wildtype. Neither genotype
393 demonstrated PPI significantly different than zero for ISIs less than or equal to 5 ms (1, 2, or 5
394 ms ISIs), suggesting lack of detection at these ISIs (B6: 1 ms $p = 0.50$, 2 ms $p = 0.51$, 5 ms $p =$
395 0.07 ; *Fmr1*: 1ms $p = 0.13$, 2 ms $p = 0.50$, 5 ms $p = 0.27$). *Fmr1* animals did not have PPI
396 significantly different from zero for ISIs of 10 ($p = 0.079$), 20 ($p = 0.05$), 30 ($p = 0.068$), 40 ($p =$
397 0.06), and 300 ($p = 0.059$) ms also suggesting potential impaired detection at these ISIs. In
398 addition, *Fmr1* mice showed increased latencies to startle at ISIs that elicited a PPI above zero,
399 suggesting that addition of a detectable prepulse actually slowed responses in comparison to B6
400 mice. Based on the results of this task and the gap detection, it was determined that the optimal
401 ISI for spatial tasks for B6 mice is 20 ms consistent with other studies (Allen and Ison, 2010).

402

403 *Experiment 3b: Minimum Audible Angle Detection with a fixed ISI*

404 To determine whether *Fmr1* mice have impairments in spatial acuity, we measured and
405 compared minimum audible angle detection for *Fmr1* and wildtype mice. The minimum audible
406 angle is defined as the smallest change in speaker source location that the animals could just
407 detect via the PPI metric (PPI significantly different than zero). In this task, the angle of the
408 speaker swap across the midline was varied as the prepulse to the startle, with a constant ISI of
409 20 ms as established by the previous experiments. 25 mice (11 B6 and 14 *Fmr1*) were tested with
410 angle swaps (to the left and right of the animal) of 7.5, 15, 30, 45 and 90° across the midline (i.e.
411 with the animal oriented towards 0° ; Figure 5A). Data were comparable for left to right and right
412 to left directional swaps, therefore the data were pooled for both directions (Figure 5B, C). There
413 was no main effect of genotype in this task ($p = 0.7255$). *Fmr1* mice showed less PPI than B6
414 mice only at the 90° angle speaker swap suggesting minimum audible detection was comparable

415 in the two groups (Figure 5B). Neither genotype showed PPI significantly different than zero for
416 angles of 30° or lower (except for at 15° where *Fmr1* mice show PPI > 0, $p = 0.026$) suggesting
417 that at these angles the animals could not detect the speaker swap, and that the animal's
418 minimum audible angles were < ~45° (B6: 7.5° $p = 0.75$, 15° $p = 0.19$, 30° $p = 0.89$; *Fmr1*: 7.5°
419 $p = 0.15$, 30° $p = 0.41$). These data suggest that both genotypes have poor angular discrimination
420 abilities as assessed in this task; however, *Fmr1* mice had longer latencies to startle at all angles
421 compared to B6 mice (Figure 4C, main effect $p < 0.0001$), consistent with results in the previous
422 varying ISI experiment.

423

424 *Experiment 4a: Auditory Spatial Release from Masking Threshold- Signal Detection in Noise*

425 Listening to sounds in a complex auditory environment with competing sound sources
426 (spatial release from masking) more naturally replicates real-world listening environments, in
427 which both people and mice with FXS experience difficulties. We used a PPI-based task to
428 replicate this experience, and to determine whether *Fmr1* mice have impairments in spatial
429 release from masking (SRM). First, we determined the signal attenuation required for animals to
430 no longer be able to distinguish signals from the background. Signal detection thresholds were
431 measured in 32 animals (16 B6 and 16 *Fmr1*) placed in the chamber with a 70 dB SPL masker
432 sound presented from the 0° speaker and a the prepulse cue centered around 4 kHz was played at
433 varying attenuated levels (from ~83.5 dB SPL) from the adjacent speakers (7.5° to the left or
434 right; Figure 6A). A tone-based sound was chosen because it is audible to the animal while not
435 eliciting a social or emotional response (such as vocalization sounds etc.) that might elicit an
436 unexpected behavioral response. In this task, there was no main effect of genotype ($p = 0.2786$).
437 At the loudest levels (9-15 dB attenuation) the 4 kHz sound elicited a robust PPI in both
438 genotypes, although *Fmr1* mice showed less PPI of their startle response compared to B6 mice
439 (Figure 6B). Both genotypes did not have PPI greater than zero at 27 dB attenuation (B6: $p =$
440 0.31 , *Fmr1*: $p = 0.22$) and B6 animals also at 24 dB attenuation ($p = 0.22$), suggesting that mice
441 did not detect the prepulse at these levels, and that their detection threshold was < 21 - 24 dB
442 attenuation. Similar to latencies in the gap detection task, B6 mice showed modulation of their
443 latency based on condition, whereas *Fmr1* mice had consistent slower latencies across conditions
444 (Figure 6C, main effect genotype $p = 0.001189$).

445

446 *Experiment 4b: Spatial Release from Masking Varying Angle*

447 Next, in order to determine if *Fmr1* mice had impairments in their spatial release from
448 masking, the angular separation between masker and prepulse signal were varied. In this task, 31
449 animals (15 B6 and 16 *Fmr1*) were presented with the same 4 kHz signal (prepulse), at 2
450 attenuation levels (15 and 24 dB attenuation), at varying angles relative to a masker noise
451 presented from the 0° speaker (Figure 7A). There was no main effect of genotype at either 15 dB
452 attenuation ($p = 0.1267$) or 24 dB attenuation ($p = 0.6325$). Consistent with the speaker swap
453 task, *Fmr1* mice only showed a difference in PPI relative to B6 mice at the largest angle (90°),
454 and only at the louder (15 dB attenuation) level ($p < 0.05$, Figure 7B, C). Both *Fmr1* and B6
455 mice showed PPI greater than zero at all angles for the louder signal (15 dB attenuation, $p > 0.05$),
456 suggesting the signal was readily detected above the masker at all angles, and only showed PPI
457 greater than zero for the largest angle (90°) for the quieter signal (24 dB attenuation) ($p < 0.05$
458 at 90° and $p > 0.05$ for all other angles for both genotypes). Similar to the above experiments, *Fmr1*
459 mice had longer latencies to startle compared to B6 mice at several angles (7.5 and 30° at 15 dB
460 attenuation and 7.5, 22.5, 30, 45° at 24 dB attenuation Figure 7D, E, main effect genotype $p =$

461 0.0001). These data do not indicate substantial deficits in SRM; however, the longer latencies
462 seen here, and in other experiments, suggests altered timing of startle responses in *Fmr1* mice
463 compared to wildtype.

464

465 *Habituation of the Startle Response*

466 Previous studies have shown that *Fmr1* mice have impaired habituation (decreased startle
467 response or PPI in later presentations of a replicate) during PPI tasks (Nielsen et al., 2002).
468 Therefore, we used the replicate number per condition (ISI, dB, etc.) as the main effect variable
469 per genotype. In contrast to previous studies, we found no habituation in either the B6 or *Fmr1*
470 knockout mice in any of the experiments tested (startle threshold, gap detection, speaker swaps,
471 or spatial release from masking)(Nielsen et al., 2002). This was indicated as no change in startle
472 amplitude or PPI as a result of replicate, in particular the second replicate compared to the last
473 replicate per condition block ($p > 0.05$ in all tests).

474

475 **Discussion**

476 We characterize the binaural and spatial hearing ability of *Fmr1* mice using a reflexive
477 PPI task. In addition, we measured the audiogram of mice using the auditory brainstem response
478 (ABR). Surprisingly, *Fmr1* mice appear to show spatial hearing ability comparable to wildtype,
479 with only subtle differences noted in some prepulse conditions. *Fmr1* mice showed similar
480 “detection” ability (PPI greater than zero) of prepulses under most conditions compared to
481 wildtype, except for varying ISI with 90° swap. In contrast, *Fmr1* mice had increased latency to
482 startle in all experiments except when determining the startle threshold. These data suggest that
483 perhaps *Fmr1* mice do not have a severe spatial hearing deficit but do show impairments in
484 timing of responses. Lastly, we did not see any short-term habituation response within
485 experiments.

486

487 *Increased high frequency ABR thresholds*

488 *Fmr1* mice had somewhat increased ABR thresholds at 16 kHz compared to B6
489 indicating potential high-frequency hearing loss. Previous studies examining ABR in *Fmr1* mice,
490 saw no change in latency of the ABR waveforms and a reduction in wave I amplitude (El-Hassar
491 et al., 2019; Rotschafer et al., 2015). One study saw an increase in ABR threshold (though across
492 all frequencies) in *Fmr1* mice (Rotschafer et al., 2015), while the other saw no change in ABR
493 threshold based on frequency (El-Hassar et al., 2019). However, both of these previous ABR
494 studies were performed in the *Fmr1* FVB knockout strain, which is one potential reason to
495 explain the difference in results with our study. In addition, the mice used in our study were
496 slightly older, average age of 125 days old for both genotypes, though we did not see any
497 obvious age-related hearing loss in either genotype (as indicated by reduced thresholds overall
498 across frequencies). Lastly, these ABR experiments were performed independently of the PPI
499 experiments described elsewhere in this study, therefore it is difficult to know if the results found
500 here are directly related to changes we see in PPI.

501

502 *No change in overall startle threshold*

503 Our results indicate that there is no difference in the overall acoustic startle response
504 between *Fmr1* mice and B6 mice. However, startle force, accounting for the weight of the mice,
505 did show differences at 100 and 110 dB SPL suggesting that *Fmr1* mice startle with less force.
506 Accounting for mass of an animal could help interpretation of data across experimental methods

507 and apparatuses (Grimsley et al., 2015). None of the previous studies account for weight or force
508 of the animal and the results in *Fmr1* mice are equivocal, where some studies show an increase
509 in the ASR (Arsenault et al., 2016; Nielsen et al., 2002), while others show a decrease in the
510 ASR (Baker et al., 2010; Chen and Toth, 2001; Frankland et al., 2004; Paylor et al., 2008;
511 Spencer et al., 2006; Thomas et al., 2012; Veeraragavan et al., 2012; Yun et al., 2006; and
512 Nielsen et al., 2002), and others show no change in overall ASR (Ding et al., 2014) consistent
513 with our study. The cause of these discrepancies is not clear; however, one possible explanation
514 is the use of different mouse strains between previous studies (Bullock et al., 1997). Additional
515 differences across reports include experimental set up and method of measuring the ASR.

516 Studies comparing patients with FXS and neurotypical human subjects did not find any
517 differences in startle magnitude (Hessl et al., 2009; Frankland et al., 2004) consistent with our
518 results. Lastly, studies have shown that the ASR is related directly to FMRP expression (Yun et
519 al., 2006) and can be rescued with addition of the *Fmr1* gene (Paylor et al., 2008) suggesting that
520 some aspects of the ASR are directly related to loss of FMRP.

521

522 *Fmr1* mice show decreased PPI during 10 and 20 ms gaps

523 Gap detection ability is thought to be directly related to E/I balance in the auditory
524 system, particularly in the inferior colliculus (IC, Sturm et al., 2017). E/I imbalances have been
525 found in *Fmr1* mice in the auditory brainstem, particularly the medial nucleus of the trapezoid
526 body (MNTB, McCullagh et al., 2017; Rotschafer et al., 2015) and lateral superior olive (LSO,
527 Garcia-Pino et al., 2017). These areas also contribute to the PPI and ASR pathways as they
528 convey sound location information to higher areas such as the IC (Koch, 1999). Our data show
529 that *Fmr1* mice show lower PPI at short gap lengths (10 and 20ms) suggesting that *Fmr1* mice
530 have impairments in their inhibition of the startle response. However, gap detection is dependent
531 on high-frequency hearing ability, and as indicated by the ABR audiogram, *Fmr1* mice have
532 higher ABR thresholds at 16 kHz compared to B6 (Fitzgibbons and Gordon-Salant, 1987). High
533 frequency hearing difficulties could help explain some of the deficits that we see in the *Fmr1*
534 knockout mice. In addition, our study examined latency to startle, and interestingly, *Fmr1* mice
535 did not show the reduction in startle latency at gap ISIs longer than 20ms observed in wildtype
536 mice.

537

538 *Fmr1* mice show decreased PPI to 90° speaker swap

539 This is the first study to measure the minimum audible angle detection of *Fmr1* mice.
540 *Fmr1* mice showed less PPI at any ISI with a 90° speaker swap indicating that they had overall
541 lower magnitude startle responses even at such a large angle than wildtype (only significantly
542 different from wildtype at 20 and 30 ms). In addition, when we kept the ISI at 20 ms and varied
543 the angle, *Fmr1* mice again showed lower PPI values at 90° speaker swaps compared to B6
544 mice. There was no difference in pinna morphology, which is one possible explanation for the
545 differences seen in 90° speaker swaps. However, both genotypes showed low PPI values for
546 other speaker angles suggesting that these mice exhibit poor minimum audible angle ability.
547 Other studies have shown higher PPI values for mice at smaller angle swaps than we report,
548 however differences in background strain (CBA/CaJ and CBA/129) and stimuli presented (wide-
549 band noise vs. high-pass noise (> 4 kHz)) may explain the differing results (Allen and Ison,
550 2010; Lauer et al., 2011). Moreover, the upper frequency of noise we used was ~20 kHz. In
551 addition, consistent with other experiments reported here, the *Fmr1* mice responded with longer
552 latencies to startle at almost all angles compared to B6. This indicates that not only do *Fmr1*

553 mice have difficulties in inhibiting their startle response, *Fmr1* mice may have longer processing
554 speeds than B6 mice.

555

556 *Fmr1* mice show alterations to spatial release from masking

557 Spatial release from masking involves detecting a signal in a noisy background. We show
558 that even at loud signals compared to background, *Fmr1* mice show less PPI of their startle
559 response than B6. In addition, when varying the location of the signal, at the louder sound, mice
560 again had deficits at 90°, but this time off to the side of the animal. Lastly, similar to the speaker
561 swap experiments, *Fmr1* animals also had longer latencies under most conditions to respond to
562 the startle speaker compared to B6, suggesting again not only impairments in detection, but also
563 reaction ability/time.

564 Other studies have examined PPI while varying the intensity of a prepulse signal above
565 an ambient noise level. While not exactly the same as the SRM task discussed here, in contrast to
566 our results, most studies found that *Fmr1* mice had increased PPI compared to wildtype (Baker et
567 al., 2010; Chen and Toth, 2001; Frankland et al., 2004; Nielsen et al., 2002; Paylor et al., 2008;
568 Veeraragavan et al., 2012), however see also (Spencer et al., 2006; Thomas et al., 2012). These
569 discrepancies could be due to the prepulse eliciting a startle response in these other studies,
570 which would cause increased PPI during the actual startle, and in particular since these studies
571 did not explore latency to startle, the prepulse startle response could be delayed coinciding with
572 the startle-eliciting speaker. Lastly, most of the other studies do not discuss where the signal is
573 coming from, which could impact the inhibition of the startle response in these animals and is
574 likely different from our experiments. Interestingly, our results are consistent with data from
575 patients with FXS who show reduced PPI under similar conditions (Frankland et al., 2004; Hessel
576 et al., 2009). Consistency with human data implies that our assay may be a better measure of PPI
577 that could apply to drug rescue experiments and be more applicable to the human FXS condition.

578

579 *Mice in these experiments did not habituate*

580 Often animals habituate to the startle stimulus, meaning that as the animal continues to be
581 exposed to a loud sound stimulus, they will no longer startle as robustly as the earlier
582 presentations of the stimulus. Habituation can also limit the length of experiments since animals
583 may not respond as robustly after several hours of testing. Interestingly, we did not see any
584 habituation to the startle in either *Fmr1* or B6 animals, as seen by a change in PPI or startle
585 amplitude between early and later presentations of the same stimulus for any of the tasks
586 presented. Other studies have examined habituation and shown that *Fmr1* mice do not habituate,
587 though their results were not consistent between an F1 cross of genotypes and *Fmr1* mice on a
588 B6 background suggesting that their results might be a result of background genotype (Nielsen et
589 al., 2002). Mice typically show less habituation than other animals, responding robustly and
590 consistently to many stimulus presentations, and habituation can be extinguished with a few
591 minutes rest between experiments (Valsamis and Schmid, 2011). Our results suggest also that
592 mice can tolerate several hours (we kept total testing time under three hours) of testing without a
593 concern for habituation to the startle response, in particular in the B6 background strain tested
594 here.

595

596 *Latency versus Startle*

597 In contrast to PPI and ASR responses that differed between *Fmr1* and B6 mice, where we
598 saw specific impairments under certain conditions, there was an overall trend for *Fmr1* mice to

599 have increased latency to startle under a variety of conditions. This could be due to impairments
600 in a different circuit that causes the response to the startle, i.e. when versus how much to startle
601 in *Fmr1* mice. There has been one study which examined latency to react in patients with FXS
602 after an acoustic startle, and they saw no differences between neurotypical controls and FXS
603 patients (Roberts et al., 2013). This study, however, did not use PPI as a measure or look at EMG
604 responses to the acoustic startle. None of the other studies examining PPI and ASR in *Fmr1* mice
605 or humans examined the latency to respond making it difficult to know if our results are
606 comparable. More in depth gap detection experiments and a more thorough ABR
607 characterization could shed light on the latency changes seen here in this study, though
608 Rotschafer et al 2015 did not see any changes to latency of the ABR (however in a different
609 background strain- FVB). In addition, the circuit underlying latency to respond to ASR or PPI is
610 not well understood and is an interesting area for further exploration.

611

612 *Conclusions*

613 Several recent studies described anatomical alterations in the sound localization pathway of
614 *Fmr1* mice which lead to altered physiological properties (Brown et al., 2010; Curry et al., 2018;
615 El-Hassar et al., 2019; Garcia-Pino et al., 2017; Lu, 2019; McCullagh et al., 2017; Rotschafer et
616 al., 2015; Rotschafer and Cramer, 2017; Strumbos et al., 2010). These alterations include
617 differences in synaptic strength and connectivity, differences in postsynaptic ion channels,
618 postsynaptic input resistance, altered firing properties, alterations in action potential shape, and
619 differences in macroscopic physiological properties such as auditory brain stem responses
620 (ABRs). In a circuit in which amplitude, kinetics and timing of excitation and inhibition are
621 balanced very precisely to perform sound localization, these alterations should have dramatic
622 effects on the animal's localization ability. Surprisingly, the observed effects were smaller than
623 expected and do not support the view of a degraded localization circuit "across the board".
624 However, our results are consistent with observations from human FXS patients, suggesting that
625 the *Fmr1* mouse model can recapitulate the human FXS condition well, at least as far as the
626 sound localization circuit is concerned.

627

628 **References**

- 629 Allen PD, Ison JR (2010) Sensitivity of the mouse to changes in azimuthal sound location:
630 Angular separation, spectral composition, and sound level. *Behav Neurosci* 124:265–277.
- 631 Anbuhl KL, Benichoux V, Greene NT, Brown AD, Tollin DJ (2017) Development of the head,
632 pinnae, and acoustical cues to sound location in a precocial species, the guinea pig (*Cavia*
633 *porcellus*). *Hear Res* 356:35–50.
- 634 Arsenault J, Gholizadeh S, Niibori Y, Pacey LK, Halder SK, Koxhioni E, Konno A, Hirai H,
635 Hampson DR (2016) FMRP Expression Levels in Mouse Central Nervous System
636 Neurons Determine Behavioral Phenotype. *Hum Gene Ther* 27:982–996.
- 637 Baker KB, Wray SP, Ritter R, Mason S, Lanthorn TH, Savelieva KV (2010) Male and female
638 *Fmr1* knockout mice on C57 albino background exhibit spatial learning and memory
639 impairments. *Genes Brain Behav* 9:562–574.
- 640 Baranek GT, Chin YH, Hess LMG, Yankee JG, Hatton DD, Hooper SR (2002) Sensory
641 processing correlates of occupational performance in children with fragile X syndrome:
642 preliminary findings. *Am J Occup Ther Off Publ Am Occup Ther Assoc* 56:538–546.

- 643 Baranek GT, Roberts JE, David FJ, Sideris J, Mirrett PL, Hatton DD, Bailey DBJ (2008)
644 Developmental trajectories and correlates of sensory processing in young boys with
645 fragile X syndrome. *Phys Occup Ther Pediatr* 28:79–98.
- 646 Bates D, Mächler M, Bolker B, Walker S (2014) Fitting Linear Mixed-Effects Models using
647 lme4. [arXiv.org](https://arxiv.org/abs/1406.5830).
- 648 Benichoux V, Ferber A, Hunt S, Hughes E, Tollin D (2018) Across Species “Natural Ablation”
649 Reveals the Brainstem Source of a Noninvasive Biomarker of Binaural Hearing. *J*
650 *Neurosci* 38:8563–8573.
- 651 Beutelmann R, Laumen G, Tollin D, Klump GM (2015) Amplitude and phase equalization of
652 stimuli for click evoked auditory brainstem responses. *J Acoust Soc Am* 137:EL71–
653 EL77.
- 654 Bronkhorst AW (2015) The cocktail-party problem revisited: early processing and selection of
655 multi-talker speech. *Atten Percept Psychophys* 77:1465–1487.
- 656 Brown MR, Kronengold J, Gazula V-R, Chen Y, Strumbos JG, Sigworth FJ, Navaratnam D,
657 Kaczmarek LK (2010) Fragile X mental retardation protein controls gating of the
658 sodium-activated potassium channel Slack. *Nat Neurosci* 13:819–821.
- 659 Bullock AE, Slobe BS, Vizquez V, Collins AC (n.d.) Inbred Mouse Strains Differ in the
660 Regulation of Startle and Prepulse Inhibition of the Startle Response 8.
- 661 Caird D, Klinke R (1983) Processing of binaural stimuli by cat superior olivary complex
662 neurons. *Exp Brain Res* 52:385–399.
- 663 Chen L, Toth M (2001) Fragile X mice develop sensory hyperreactivity to auditory stimuli.
664 *Neuroscience* 103:1043–1050.
- 665 Cherry EC (1953) Some Experiments on the Recognition of Speech, with One and with Two
666 Ears. *J Acoust Soc Am* 25:975–979.
- 667 Consortium TD-BFX et al. (1994) *Fmr1* knockout mice: A model to study fragile X mental
668 retardation. *Cell* 78:23–33.
- 669 Contractor A, Klyachko VA, Portera-Cailliau C (2015) Altered Neuronal and Circuit Excitability
670 in Fragile X Syndrome. *Neuron* 87:699–715.
- 671 Curry RJ, Peng K, Lu Y (2018) Neurotransmitter- and Release-Mode-Specific Modulation of
672 Inhibitory Transmission by Group I Metabotropic Glutamate Receptors in Central
673 Auditory Neurons of the Mouse. *J Neurosci* 38:8187–8199.
- 674 Ding Q, Sethna F, Wang H (2014) Behavioral analysis of male and female *Fmr1* knockout mice
675 on C57BL/6 background. *Behav Brain Res* 271:72–78.
- 676 El-Hassar L, Song L, Winston TJT, Large CH, Alvaro G, Santos-Sacchi J, Kaczmarek LK
677 (2019) Modulators of Kv3 potassium channels rescue the auditory function of Fragile X
678 mice. *J Neurosci* 0839–18.
- 679 Feng AS, Ratnam R (2000) Neural Basis of Hearing in Real-World Situations. *Annu Rev*
680 *Psychol* 51:699–725.
- 681 Ferber AT, Benichoux V, Tollin DJ (2016) Test-Retest Reliability of the Binaural Interaction
682 Component of the Auditory Brainstem Response. *Ear Hear* 37:e291-301.
- 683 Fitzgibbons PJ, Gordon-Salant S (1987) Temporal gap resolution in listeners with high-
684 frequency sensorineural hearing loss. *J Acoust Soc Am* 81:133–137.
- 685 Frankland PW, Wang Y, Rosner B, Shimizu T, Balleine BW, Dykens EM, Ornitz EM, Silva AJ
686 (2004) Sensorimotor gating abnormalities in young males with fragile X syndrome and
687 *Fmr1*-knockout mice. *Mol Psychiatry* 9:417–425.

- 688 Garcia-Pino E, Gessele N, Koch U (2017) Enhanced Excitatory Connectivity and Disturbed
689 Sound Processing in the Auditory Brainstem of Fragile X Mice. *J Neurosci Off J Soc*
690 *Neurosci* 37:7403–7419.
- 691 Goldberg JM, Brown PB (1969) Response of binaural neurons of dog superior olivary complex
692 to dichotic tonal stimuli: some physiological mechanisms of sound localization. *J*
693 *Neurophysiol* 32:613–636.
- 694 Greene NT, Anbuhl KL, Ferber AT, DeGuzman M, Allen PD, Tollin DJ (2018) Spatial hearing
695 ability of the pigmented Guinea pig (*Cavia porcellus*): Minimum audible angle and
696 spatial release from masking in azimuth. *Hear Res* 365:62–76.
- 697 Grimsley CA, Longenecker RJ, Rosen MJ, Young JW, Grimsley JM, Galazyuk AV (2015) An
698 improved approach to separating startle data from noise. *J Neurosci Methods* 253:206–
699 217.
- 700 Grothe B, Pecka M, McAlpine D (2010) Mechanisms of sound localization in mammals. *Physiol*
701 *Rev* 90:983–1012.
- 702 Hessl D, Berry-Kravis E, Cordeiro L, Yuhas J, Ornitz EM, Campbell A, Chruscinski E, Hervey
703 C, Long JM, Hagerman RJ (2009) Prepulse inhibition in fragile X syndrome: Feasibility,
704 reliability, and implications for treatment. *Am J Med Genet B Neuropsychiatr Genet*
705 150B:545–553.
- 706 Keine C, Rübsamen R, Englitz B (2016) Inhibition in the auditory brainstem enhances signal
707 representation and regulates gain in complex acoustic environments. *eLife* 5.
- 708 Koch M (1999) The neurobiology of startle. *Prog Neurobiol* 59:107–128.
- 709 Kuznetsova A, Brockhoff PB, Christensen RHB (2017) **lmerTest** Package: Tests in Linear
710 Mixed Effects Models. *J Stat Softw* 82.
- 711 Lauer AM, Slee SJ, May BJ (2011) Acoustic Basis of Directional Acuity in Laboratory Mice. *J*
712 *Assoc Res Otolaryngol* 12:633–645.
- 713 Lenth R (2019) emmeans: Estimated Marginal Means, aka Least-Squares Means.
- 714 Lu Y (2019) Subtle differences in synaptic transmission in medial nucleus of trapezoid body
715 neurons between wild-type and *Fmr1* knockout mice. *Brain Res* 1717:95–103.
- 716 McCullagh EA, Salcedo E, Huntsman MM, Klug A (2017) Tonotopic alterations in inhibitory
717 input to the medial nucleus of the trapezoid body in a mouse model of Fragile X
718 syndrome. *J Comp Neurol* 262:375.
- 719 Moore MJ, Caspary DM (1983) Strychnine blocks binaural inhibition in lateral superior olivary
720 neurons. *J Neurosci Off J Soc Neurosci* 3:237–242.
- 721 Nielsen DM, Derber WJ, McClellan DA, Crnic LS (2002) Alterations in the auditory startle
722 response in *Fmr1* targeted mutant mouse models of fragile X syndrome. *Brain Res*
723 927:8–17.
- 724 Paylor R, Yuva-Paylor LA, Nelson DL, Spencer CM (2008) Reversal of sensorimotor gating
725 abnormalities in *Fmr1* knockout mice carrying a human *Fmr1* transgene. *Behav Neurosci*
726 122:1371–1377.
- 727 Penagarikano O, Mulle JG, Warren ST (2007) The Pathophysiology of Fragile X Syndrome.
728 *Annu Rev Genomics Hum Genet* 8:109–129.
- 729 Pollak GD, Burger RM, Park TJ, Klug A, Bauer EE (2002) Roles of inhibition for transforming
730 binaural properties in the brainstem auditory system. *Hear Res* 168:60–78.
- 731 R Core Team (2013) R: A Language and Environment for Statistical Computing. Vienna,
732 Austria: R Foundation for Statistical Computing.

- 733 Roberts JE, Long ACJ, McCary LM, Quady AN, Rose BS, Widrick D, Baranek G (2013)
734 Cardiovascular and Behavioral Response to Auditory Stimuli in Boys With Fragile X
735 Syndrome. *J Pediatr Psychol* 38:276–284.
- 736 Rogers SJ, Hepburn S, Wehner E (2003) Parent reports of sensory symptoms in toddlers with
737 autism and those with other developmental disorders. *J Autism Dev Disord* 33:631–642.
- 738 Rotschafer SE, Cramer KS (2017) Developmental Emergence of Phenotypes in the Auditory
739 Brainstem Nuclei of Fmr1 Knockout Mice. *eNeuro* 4:1–21.
- 740 Rotschafer SE, Marshak S, Cramer KS (2015) Deletion of Fmr1 Alters Function and Synaptic
741 Inputs in the Auditory Brainstem. *PLoS One* 10:1–15.
- 742 Rotschafer SE, Razak KA (2014) Auditory processing in fragile x syndrome. *Front Cell*
743 *Neurosci* 8:19.
- 744 Ruby K, Falvey K, Kulesza RJ (2015) Abnormal neuronal morphology and neurochemistry in
745 the auditory brainstem of Fmr1 knockout rats. *Neuroscience* 303:285–298.
- 746 Spencer CM, Serysheva E, Yuva-Paylor LA, Oostra BA, Nelson DL, Paylor R (2006)
747 Exaggerated behavioral phenotypes in Fmr1/Fxr2 double knockout mice reveal a
748 functional genetic interaction between Fragile X-related proteins. *Hum Mol Genet*
749 15:1984–1994.
- 750 Strumbos JG, Brown MR, Kronengold J, Polley DB, Kaczmarek LK (2010) Fragile X Mental
751 Retardation Protein Is Required for Rapid Experience-Dependent Regulation of the
752 Potassium Channel Kv3.1b. *J Neurosci* 30:10263–10271.
- 753 Sturm JJ, Zhang-Hooks Y-X, Roos H, Nguyen T, Kandler K (2017) Noise Trauma-Induced
754 Behavioral Gap Detection Deficits Correlate with Reorganization of Excitatory and
755 Inhibitory Local Circuits in the Inferior Colliculus and Are Prevented by Acoustic
756 Enrichment. *J Neurosci* 37:6314–6330.
- 757 Thomas AM, Bui N, Perkins JR, Yuva-Paylor LA, Paylor R (2012) Group I metabotropic
758 glutamate receptor antagonists alter select behaviors in a mouse model for fragile X
759 syndrome. *Psychopharmacology (Berl)* 219:47–58.
- 760 Thompson AM, Schofield BR (2000) Afferent projections of the superior olivary complex.
761 *Microsc Res Tech* 51:330–354.
- 762 Valsamis B, Schmid S (2011) Habituation and Prepulse Inhibition of Acoustic Startle in
763 Rodents. *J Vis Exp*.
- 764 Veeraragavan S, Graham D, Bui N, Yuva-Paylor LA, Wess J, Paylor R (2012) Genetic reduction
765 of muscarinic M4 receptor modulates analgesic response and acoustic startle response in
766 a mouse model of fragile X syndrome (FXS). *Behav Brain Res* 228:1–8.
- 767 Wang T, de Kok L, Willemsen R, Elgersma Y, Borst JGG (2015) In vivo synaptic transmission
768 and morphology in mouse models of Tuberous sclerosis, Fragile X syndrome,
769 Neurofibromatosis type 1, and Costello syndrome. *Front Cell Neurosci* 9:234.
- 770 Wang Y, Sakano H, Beebe K, Brown MR, de Laat R, Bothwell M, Kulesza RJ, Rubel EW
771 (2014) Intense and specialized dendritic localization of the fragile X mental retardation
772 protein in binaural brainstem neurons: A comparative study in the alligator, chicken,
773 gerbil, and human: FMRP localization in NL/MSO dendrites. *J Comp Neurol* 522:2107–
774 2128.
- 775 Wickham H (2016) *ggplot2: Elegant Graphics for Data Analysis*. Springer-Verlag New York.
- 776 Young JS, Fechter LD (1983) Reflex inhibition procedures for animal audiometry: a technique
777 for assessing ototoxicity. *J Acoust Soc Am* 73:1686–1693.

778 Yun S-W, Platholi J, Flaherty MS, Fu W, Kottmann AH, Toth M (2006) *Fmrp* is required for the
779 establishment of the startle response during the critical period of auditory development.
780 *Brain Res* 1110:159–165.

781 Zorio DAR, Jackson CM, Liu Y, Rubel EW, Wang Y (2017) Cellular distribution of the fragile
782 X mental retardation protein in the mouse brain: *Fmrp* distribution in the mouse brain. *J*
783 *Comp Neurol* 525:818–849.

784
785 **Fig 1. Increased auditory ABR threshold in *Fmr1* mice at 16kHz compared to B6 mice.**
786 Tonal ABR measurements were made on mice at 3 frequencies, 4000, 8000, and 16000Hz.
787 There were no differences in ABR auditory thresholds at 4000 and 8000Hz between *Fmr1* and
788 B6 mice. However, at 16kHz *Fmr1* mice had increased thresholds compared to B6. ** $p < 0.01$
789

790 **Fig 2. No difference in startle amplitude or latency between B6 and *Fmr1* mice, decreased**
791 **force in *Fmr1* mice.** A, illustration of the experimental setup. Animals were placed in the center
792 of the speaker array in the presence of 70dB SPL broadband noise playing from the central
793 speaker at 0° (blue speaker). Startle eliciting stimuli were presented by an additional speaker
794 placed directly over the mouse's head (not shown). B, the animal's startle amplitude increased
795 with stimulus level (dB SPL) for both B6 (red) and *Fmr1* mice (teal). A total of 22 B6 and 14
796 *Fmr1* mice were tested in this task, with a subset (6 B6 and 8 *Fmr1*) tested below 80 dB SPL. C,
797 Force of response to the startle stimuli was smaller for *Fmr1* mice compared to B6. D, latency to
798 respond (in ms) to the startle stimulus decreased with increasing stimulus intensity (dB SPL) for
799 both B6 and *Fmr1* mice. * $p < 0.05$
800

801 **Fig 3. *Fmr1* mice have decreased PPI and increased latency to startle during a gap**
802 **detection task.** 42 mice (20 B6 and 22 *Fmr1*) were tested in a gap detection task, where a 20
803 ms quiet gap was introduced into 70dB SPL broadband noise (blue speaker at the center of the
804 array), which was presented at varying ISIs before the startle eliciting stimulus presentation (A).
805 *Fmr1* mice (teal) showed less PPI at 10 ms and 20 ms ISI compared to B6 (red; B). *Fmr1* mice
806 startle responses latencies were longer to 1, 2, 5, 40, 80, 160 and 240 ms ISIs compared to
807 wildtype (C). Boxes show conditions where PPI is not different from zero for both genotypes. *
808 $p < 0.05$, ** $p < 0.01$, *** $p < 0.001$.
809

810 **Fig 4. *Fmr1* mice have decreased PPI and increased startle latency in response to a 90°**
811 **speaker swap compared to B6.** 26 mice (12 B6, 14 *Fmr1*) were tested in a 90° angle speaker
812 swap task with varying ISI (A). *Fmr1* mice (teal) have lower PPI at 20 ms and 30 ms ISIs than
813 B6 mice (red; B). *Fmr1* mice had longer latencies to startle at all ISIs except 1 ms and 2 ms
814 compared to B6 mice. Boxes show conditions where PPI is not different from zero for both
815 genotypes. * $p < 0.05$, ** $p < 0.01$, *** $p < 0.001$.
816

817 **Fig 5. *Fmr1* mice had a reduction in PPI compared to B6 at 90° speaker swap and longer**
818 **latencies to startle in all conditions.** 25 mice (11 B6 and 14 *Fmr1*) were tested with varying
819 angles of a speaker swap, both left and right directions across the midline, and constant 20 ms
820 ISI (A, example leftward swap is shown). *Fmr1* mice (blue) show less PPI at 90° than B6 mice
821 (red; B). *Fmr1* mice had longer latencies to startle at all angle conditions compared to B6 (C).
822 Boxes show conditions where PPI is not different from zero for both genotypes. * $p < 0.05$, ***
823 $p < 0.001$.
824

825 **Fig 6. *Fmr1* mice showed less PPI of their startle, and longer latencies in some**
826 **conditions compared to B6 mice.** A signal noise was played at varying sound levels from a

827 loudspeaker offset by 7.5° from a 70 dB SPL masker noise at 0° (A). *Fmr1* mice (teal) had
 828 reduced PPI of their startle at 9, 12, and 15 dBs attenuation compared to B6 mice (red; B). *Fmr1*
 829 mice also had increased latency to startle at 9 and 24 dBs attenuation compared to B6 (C).
 830 Boxes show conditions where PPI is not different from zero for both genotypes. * p<0.05, **
 831 p<0.01, *** p<0.001.

833 **Fig 7. *Fmr1* mice had reduced PPI at 90° and 15 dB attenuation with increased latency to**
 834 **startle in several conditions compared to B6.** The signal was varied at 2 levels of attenuation
 835 (15 and 24 dB) and varied at several angles from the 70 dB SPL masker at 0° to the left or right
 836 (A). *Fmr1* mice (blue) had decreased PPI of their startle response at 90° from the masker only
 837 at 15dB attenuation compared to B6 mice (red; B, C). *Fmr1* mice had increased latency to
 838 startle at 7.5 and 30° at 15 dB attenuation (D) and 7.5, 22.5, 30, 45, 90° at 24 dB attenuation (E)
 839 compared to B6 mice. Boxes show conditions where PPI is not different from zero for both
 840 genotypes. * p<0.05, ** p<0.01, *** p<0.001.

841
 842 **Table 1:** Summary statistics for ABR measurements

Experiment	B6			Fmr1			p-value	
	Mean ± SEM	Median	IQR Q1-Q3	Mean ± SEM	Median	IQR Q1-Q3		
ABR audiogram (dB SPL)	4000	59.3 ± 3.7	55.0	55.0-65.0	61.7 ± 2.1	65.0	57.5-65.0	0.6278
	8000	39.3 ± 36.1	35.0	35.0-45.0	45.0 ± 3.7	45.0	37.5-52.5	0.2503
	16000	37.9 ± 3.6	35.0	35.0-40.0	53.3 ± 3.1	55.0	47.5-55.0	0.0040

844

845

846

847

848

849

850 **Table 2:** Summary statistics for startle threshold and PPI experiments

851

Experiment	B6			Fmr1			p-value	
	Mean ± SEM	Median	IQR Q1-Q3	Mean ± SEM	Median	IQR Q1-Q3		
Threshold (dB SPL)	60	329.0 ± 13.7	289.0	267-369	380.1 ± 36.8	312.5	272-412	0.2903
	70	387.0 ± 36.1	320.0	276-363	349.0 ± 22.3	306.0	273-360	0.0706
	80	391.0 ± 17.6	326.0	273-489	457.3 ± 37.8	320.5	266-539	0.8195
	90	633.8 ± 33.9	586.0	397-758	731.3 ± 69.2	502.5	380-869	0.5794
	100	887.0 ± 47.9	815.5	543-1187	748.4 ± 50.5	687.5	450-946	0.0583
	110	1001.9 ± 58.7	954.0	564-1297	879.0 ± 54.6	813.0	546-1099	0.0828
	120	805.2 ± 53.2	608.0	400-1220	880.7 ± 72.7	706.0	447-1146	0.7422
Gap Detection (ISI)	1	0.02 ± 0.03	-0.0008	-0.22-0.26	0.03 ± 0.03	0.06	-0.11-0.27	0.5314
	2	0.09 ± 0.03	0.08	-0.13-0.32	0.08 ± 0.02	0.11	-0.04-0.27	0.4421
	5	0.24 ± 0.02	0.26	0.05-0.43	0.19 ± 0.02	0.23	0.03-0.38	0.1026
	10	0.44 ± 0.02	0.49	0.35-0.62	0.33 ± 0.02	0.37	0.21-0.49	0.0153*

	20	0.54 ± 0.02	0.59	0.41-0.69	0.38 ± 0.02	0.42	0.26-0.56	0.0011**
	40	0.23 ± 0.02	0.24	0.10-0.41	0.18 ± 0.03	0.27	0.03-0.42	0.3753
	80	0.10 ± 0.02	0.15	-0.04-0.35	0.14 ± 0.02	0.21	0.04-0.34	0.3789
	160	0.15 ± 0.02	0.17	0.01-0.38	0.13 ± 0.02	0.19	-0.01-0.36	0.6436
	240	0.15 ± 0.02	0.06	-0.03-0.35	0.13 ± 0.02	0.19	-0.02-0.34	0.7266
90° Speaker Swap (ISI)	1	-0.05 ± 0.05	-0.04	-0.24-0.21	-0.10 ± 0.04	-0.05	-0.35-0.15	0.5659
	2	0.04 ± 0.04	0.10	-0.16-0.27	-0.04 ± 0.05	0.04	-0.28-0.27	0.3390
	5	0.12 ± 0.05	0.19	-0.14-0.43	0.07 ± 0.05	0.12	-0.13-0.31	0.5434
	10	0.27 ± 0.03	0.26	0.13-0.44	0.11 ± 0.04	0.15	-0.02-0.33	0.0823
	20	0.35 ± 0.03	0.39	0.18-0.56	0.13 ± 0.05	0.19	-0.05-0.42	0.0136*
	30	0.31 ± 0.04	0.37	0.12-0.54	0.12 ± 0.05	0.16	-0.13-0.41	0.0388*
	40	0.26 ± 0.03	0.28	0.10-0.46	0.12 ± 0.05	0.18	-0.09-0.38	0.1329
	80	0.32 ± 0.03	0.36	0.23-0.51	0.16 ± 0.04	0.24	-0.06-0.41	0.0809
	100	0.27 ± 0.04	0.32	0.09-0.48	0.20 ± 0.03	0.19	0.03-0.43	0.4565
	150	0.37 ± 0.03	0.42	0.19-0.56	0.23 ± 0.03	0.27	0.06-0.45	0.1400
300	0.25 ± 0.03	0.25	0.11-0.43	0.12 ± 0.04	0.15	-0.06-0.35	0.1571	
Speaker Swap (Angle)	7.5°	-0.01 ± 0.02	-0.008	-0.21-0.22	-0.04 ± 0.03	0.06	-0.12-0.21	0.4647
	15°	0.04 ± 0.02	0.03	-0.14-0.26	0.06 ± 0.02	0.10	-0.07-0.29	0.6043
	30°	0.005 ± 0.03	0.04	-0.18-0.23	0.02 ± 0.02	0.08	-0.12-0.26	0.6542
	45°	0.10 ± 0.03	0.17	-0.14-0.36	0.13 ± 0.02	0.17	0.010-0.37	0.3635
	90°	0.22 ± 0.02	0.24	0.08-0.40	0.12 ± 0.02	0.18	-0.01-0.37	0.0228*
Threshold SRM (dB attenuation)	9	0.40 ± 0.02	0.42	0.25-0.56	0.27 ± 0.03	0.30	0.19-0.44	0.0309*
	12	0.48 ± 0.02	0.55	0.33-0.65	0.31 ± 0.03	0.34	0.23-0.47	0.0067**
	15	0.49 ± 0.02	0.56	0.37-0.65	0.34 ± 0.02	0.36	0.23-0.51	0.0153*
	18	0.32 ± 0.03	0.32	0.21-0.47	0.29 ± 0.02	0.32	0.18-0.46	0.6152
	21	0.18 ± 0.03	0.21	0.07-0.38	0.17 ± 0.04	0.27	-0.03-0.39	0.7820
	24	0.05 ± 0.03	0.10	-0.09-0.25	0.09 ± 0.03	0.08	-0.11-0.33	0.5292
27	-0.04 ± 0.04	0.04	-0.23-0.19	0.05 ± 0.04	0.12	-0.11-0.32	0.1145	
SRM 15 dB attenuation (Angle)	7.5°	0.42 ± 0.03	0.46	0.23-0.61	0.34 ± 0.03	0.40	0.23-0.48	0.2315
	15°	0.38 ± 0.03	0.35	0.20-0.61	0.30 ± 0.03	0.33	0.17-0.49	0.2133
	22.5°	0.36 ± 0.03	0.37	0.22-0.58	0.33 ± 0.03	0.40	0.17-0.49	0.6620
	30°	0.34 ± 0.03	0.40	0.19-0.57	0.31 ± 0.02	0.35	0.21-0.47	0.6156
	45°	0.41 ± 0.03	0.45	0.23-0.61	0.31 ± 0.03	0.35	0.15-0.47	0.1220
	90°	0.42 ± 0.03	0.49	0.27-0.64	0.21 ± 0.04	0.31	0.04-0.43	0.0030**
SRM 24 dB attenuation (Angle)	7.5°	-0.02 ± 0.04	-0.002	-0.24-0.19	0.07 ± 0.04	0.11	-0.09-0.35	0.1804
	15°	-0.05 ± 0.03	0.07	-0.16-0.28	0.06 ± 0.04	0.13	-0.07-0.28	0.8865
	22.5°	-0.006 ± 0.03	0.009	-0.19-0.18	-0.02 ± 0.05	0.11	-0.16-0.30	0.8580
	30°	0.02 ± 0.04	0.07	-0.20-0.28	0.04 ± 0.04	0.08	-0.11-0.31	0.7420
	45°	0.03 ± 0.04	0.13	-0.20-0.28	0.04 ± 0.04	0.09	-0.11-0.32	0.8239
	90°	0.18 ± 0.03	0.24	0.06-0.38	0.18 ± 0.03	0.23	-0.03-0.43	0.9639

852 Values in red indicate a PPI not significantly different than zero

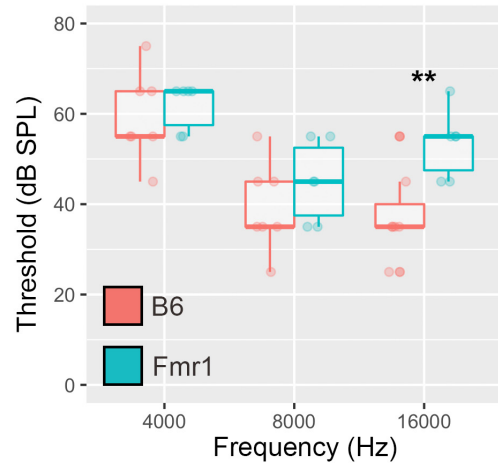
853

854 **Table 3:** Summary statistics for latency (ms)

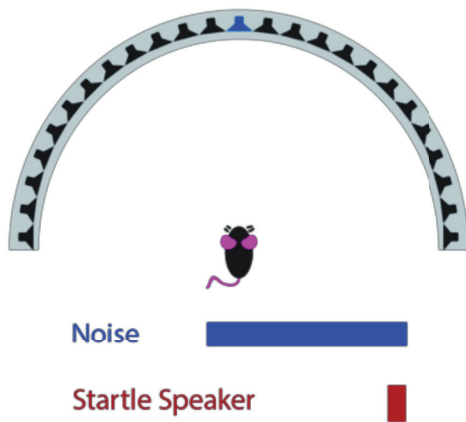
Experiment	<i>B6</i>			<i>Fmr1</i>			p-value	
	Mean \pm SEM	Median	IQR Q1-Q3	Mean \pm SEM	Median	IQR Q1-Q3		
Threshold (dB SPL)	60	47.2 \pm 5.87	47.0	21.5-75.5	45.2 \pm 7.6	47.0	18.0-63.0	0.8331
	70	41.9 \pm 5.18	35.0	22.0-73.0	34.1 \pm 6.3	26.0	15.3-41.5	0.2136
	80	36.6 \pm 2.88	32.0	20.0-48.5	35.4 \pm 3.5	32.0	18.3-43.5	0.7538
	90	25.4 \pm 1.47	24.0	19.3-32.8	26.0 \pm 1.9	24.0	18.0-33.0	0.8117
	100	25.1 \pm 1.41	22.0	20.0-30.3	26.6 \pm 2.0	24.5	21.0-32.0	0.6117
	110	25.0 \pm 1.27	22.0	20.0-27.5	26.5 \pm 1.7	24.0	20.0-31.0	0.5933
	120	26.9 \pm 1.89	22.0	17.0-33.0	27.8 \pm 2.4	23.0	18.0-34.5	0.7275
Gap Detection (ISI)	1	26.6 \pm 1.34	23.0	20.0-27.0	29.5 \pm 1.48	26.0	19.8-33.0	0.0260*
	2	26.6 \pm 1.38	23.0	17.0-29.0	30.9 \pm 1.43	28.0	20.0-35.0	0.0057**
	5	28.9 \pm 1.30	25.0	21.8-32.0	29.9 \pm 1.35	27.0	18.0-36.0	0.1541
	10	34.2 \pm 1.47	31.0	23.0-42.0	34.3 \pm 1.74	28.5	20.0-45.0	0.3521
	20	35.7 \pm 1.84	31.0	20.0-48.0	36.1 \pm 1.88	30.0	20.0-51.5	0.3142
	40	28.2 \pm 1.33	24.0	21.0-31.0	33.7 \pm 1.61	29.0	20.0-43.5	0.0006***
	80	22.5 \pm 0.53	23.0	21.0-24.3	30.4 \pm 1.58	28.0	22.0-34.3	0.0002***
	160	21.7 \pm 0.74	23.0	20.3-26.0	28.4 \pm 1.51	28.0	20.8-33.0	0.0012**
	240	21.3 \pm 0.84	22.5	19.0-25.0	32.0 \pm 1.76	28.0	22.0-34.3	<0.0001***
90° Speaker Swap (ISI)	1	23.2 \pm 1.52	22.0	21.0-24.0	26.1 \pm 1.68	25.0	22.0-32.0	0.2625
	2	21.6 \pm 0.70	22.0	20.0-24.0	28.8 \pm 2.15	26.0	21.0-33.0	0.0098
	5	22.3 \pm 1.17	22.0	20.0-24.3	29.5 \pm 2.06	25.5	22.0-36.8	0.0107*
	10	23.5 \pm 1.46	24.0	20.0-29.0	30.9 \pm 2.74	29.0	16.8-39.3	0.0100*
	20	23.0 \pm 1.23	24.0	20.8-26.0	32.7 \pm 2.78	29.0	23.0-39.0	0.0008***
	30	24.2 \pm 1.06	24.0	21.0-30.3	34.5 \pm 2.92	28.0	20.3-47.0	0.0005***
	40	24.6 \pm 1.70	24.0	22.0-31.5	32.3 \pm 2.40	30.0	22.0-40.0	0.0062**
	80	23.8 \pm 1.23	24.0	20.8-30.3	33.2 \pm 2.58	30.0	22.0-39.0	0.0013**
	100	22.3 \pm 1.38	23.0	18.5-28.3	30.7 \pm 2.87	28.0	14.0-41.0	0.0044**
	150	26.7 \pm 1.68	26.0	22.0-31.5	32.2 \pm 2.36	31.0	25.5-39.5	0.0489*
	300	23.4 \pm 1.29	24.0	21.0-28.0	32.1 \pm 2.25	29.0	29.0-23.0	0.0020**
Speaker Swap (Angle)	7.5°	21.5 \pm 0.70	22.0	21.0-23.8	30.1 \pm 1.30	27.0	22.0-34.0	<0.0001***
	15°	21.8 \pm 0.79	21.0	20.0-23.8	29.4 \pm 1.44	25.0	20.0-33.0	<0.0001***
	30°	22.0 \pm 0.76	22.0	20.0-24.0	28.0 \pm 1.22	25.0	21.0-33.0	<0.0001***
	45°	21.5 \pm 0.69	22.0	20.0-24.0	31.1 \pm 1.30	28.0	22.0-35.0	<0.0001***
	90°	24.9 \pm 0.95	23.0	21.0-27.0	31.7 \pm 1.56	27.0	20.8-35.3	<0.0001***
Threshold SRM (dB)	9	18.0 \pm 2.42	10.0	5.0-22.5	36.1 \pm 3.32	37.0	14.0-52.0	<0.0001***
	12	23.9 \pm 2.78	15.0	10.0-31.0	34.0 \pm 3.40	29.0	13.0-48.0	0.0231
	15	35.6 \pm 2.50	31.0	19.5-53.5	36.6 \pm 3.98	29.0	15.0-57.0	0.8374
	18	26.0 \pm 1.87	24.0	21.0-29.8	35.8 \pm 2.91	33.0	19.0-49.0	0.0224*

	21	25.4 ± 1.49	24.0	21.0-28.5	32.2 ± 2.92	28.5	17.5-42.0	0.0994
	24	23.4 ± 1.30	22.0	21.0-28.0	35.3 ± 2.44	31.0	24.0-45.0	0.0042**
	27	24.7 ± 1.67	22.0	21.0-25.0	30.3 ± 2.43	25.0	21.0-35.0	0.1750
SRM 15 dB attenuation (Angle)	7.5°	25.4 ± 1.82	23.5	13.3-32.0	38.3 ± 3.49	32.0	18.0-57.5	0.0008***
	15°	27.8 ± 2.13	24.0	16.5-33.0	33.0 ± 3.06	31.0	12.5-43.5	0.1969
	22.5°	24.8 ± 1.97	23.0	14.0-30.0	29.6 ± 2.66	25.5	14.0-44.0	0.2396
	30°	23.5 ± 1.88	23.0	13.0-31.0	32.0 ± 3.45	26.0	11.0-48.0	0.0288*
	45°	25.5 ± 2.02	23.0	14.0-30.8	31.8 ± 3.29	24.0	14.0-41.0	0.1131
	90°	22.5 ± 2.52	13.0	8.5-29.5	29.0 ± 2.97	18.0	11.0-47.0	0.0803
SRM 24 dB attenuation (Angle)	7.5°	23.6 ± 1.71	22.0	20.0-24.0	29.8 ± 2.33	25.0	22.0-34.0	0.0074**
	15°	25.3 ± 1.61	22.0	21.0-27.0	25.7 ± 1.98	23.5	14.0-32.0	0.5322
	22.5°	23.6 ± 1.51	22.0	21.0-24.0	32.0 ± 2.06	28.0	22.5-33.5	0.0004***
	30°	22.4 ± 1.46	22.0	21.0-24.0	30.1 ± 1.96	28.0	21.0-38.0	0.0014**
	45°	25.1 ± 1.62	22.0	20.0-27.0	30.8 ± 1.94	27.0	23.0-36.0	0.0098**
	90°	26.0 ± 1.61	24.0	24.0-29.0	26.3 ± 2.45	23.5	11.3-32.0	0.5437

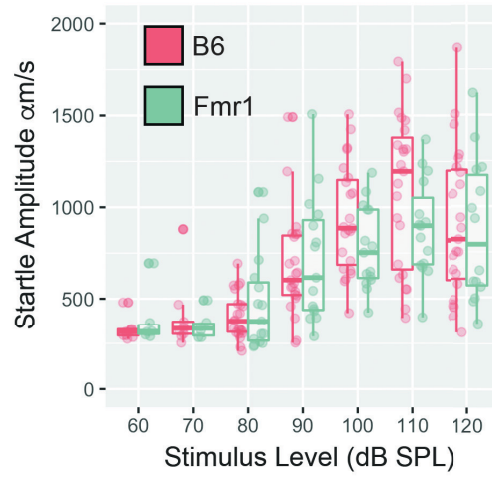
855
856
857
858
859
860
861
862
863
864
865
866
867



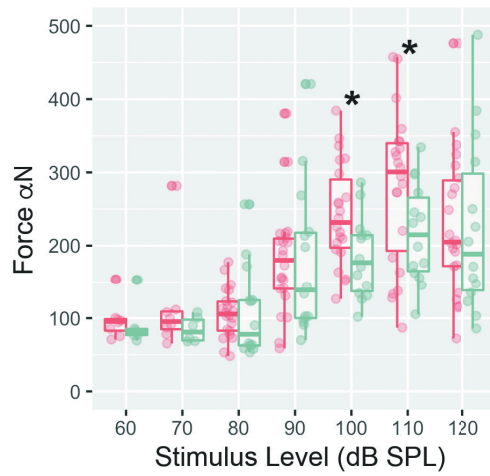
A



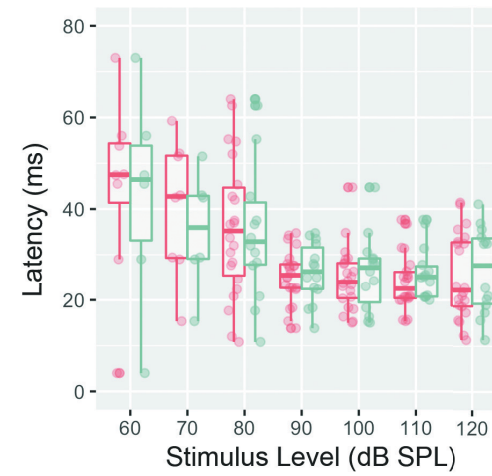
B Threshold

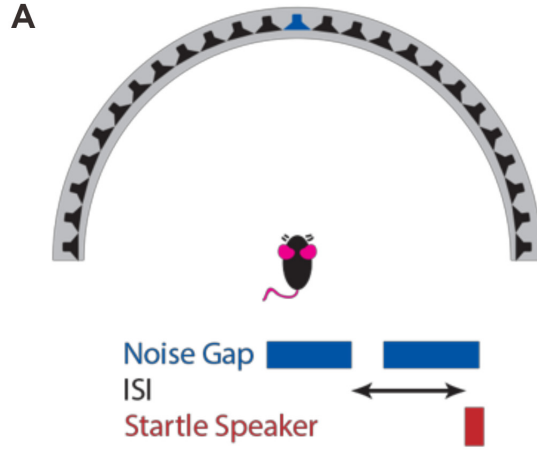


C Force Threshold

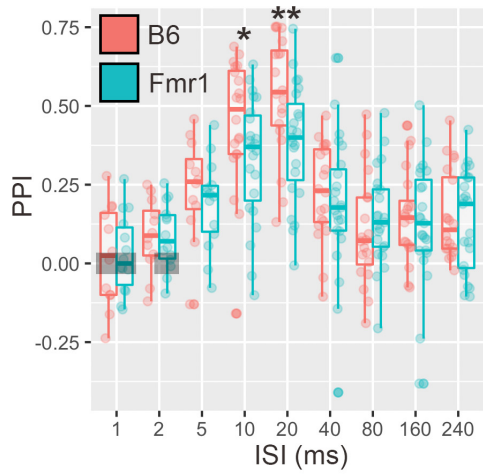


D Latency

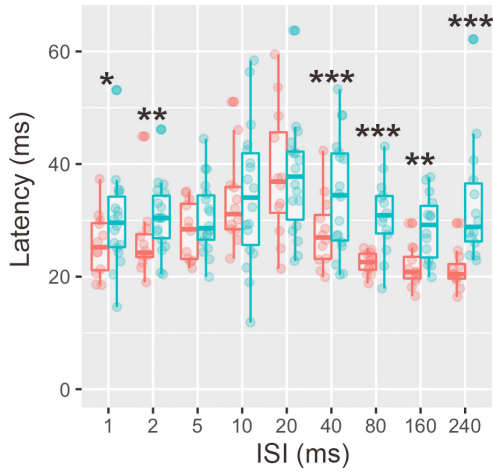


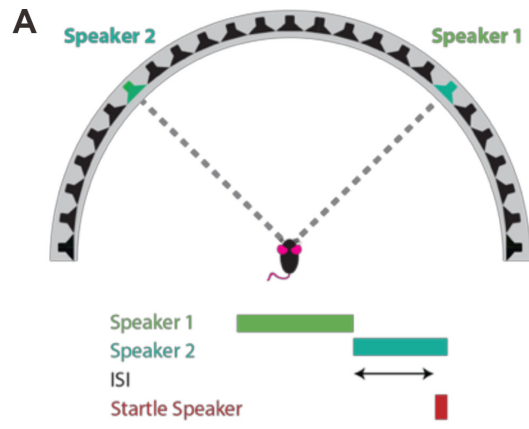


B Gap Detection

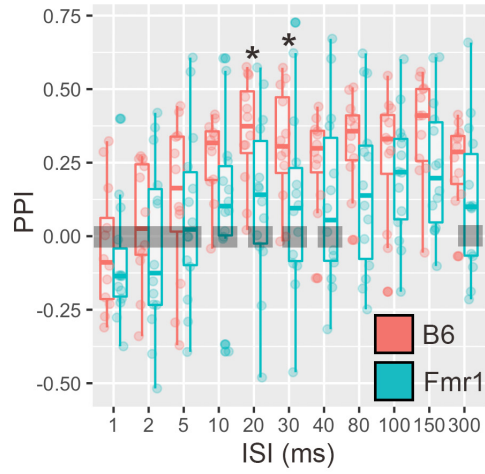


C Latency

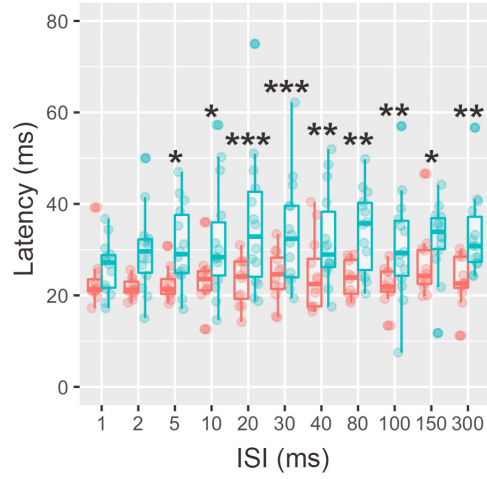


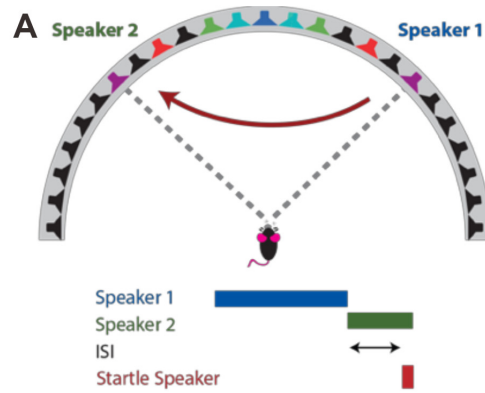


B Interstimulus Interval

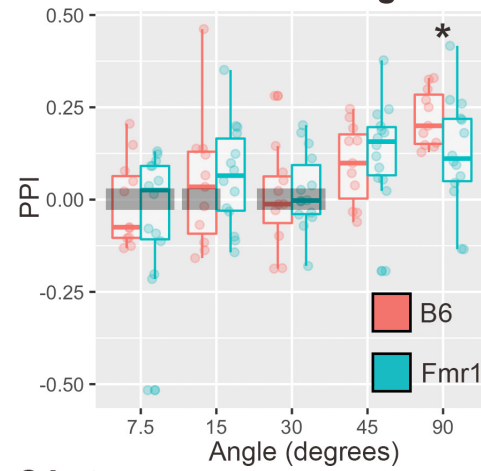


C Latency





B Minimum Audible Angle



C Latency

